Nkx2-5 defines distinct scaffold and recruitment phases during formation of the cardiac Purkinje fiber network

Caroline Choquet, Robert G. Kelly and Lucile Miquerol*

Aix-Marseille Université, CNRS UMR 7288, Developmental Biology Institute of Marseille, Campus de Luminy Case 907, 13288 Marseille Cedex 9, France; caroline.choquet@univ-amu.fr (C.C.); robert.kelly@univ-amu.fr (R.G.K.)

* Correspondence: lucile.miquerol@univ-amu.fr; Tel.: +33-413-94-24-09

Abstract

The ventricular conduction system coordinates heartbeats by rapid propagation of electrical activity through the Purkinje fiber (PF) network. PF share common progenitors with contractile cardiomyocytes, yet the mechanisms of segregation and PF network morphogenesis are unknown. Using genetic fate mapping and temporal clonal analysis we identify cardiomyocytes committed to the PF lineage as early as E7.5. A polyclonal PF network emerges by progressive recruitment of conductive precursors to this scaffold from a pool of bipotent progenitors. At late fetal stages, the segregation of conductive cells increases during a phase of rapid recruitment to build the definitive PF network. In *Nkx2-5* haploinsufficient embryos, PF differentiation is impaired leading to failure to extend the scaffold. In particular, late fetal recruitment is abolished resulting in PF hypoplasia and persistence of bipotent progenitors at birth. Our results reveal how transcription factor dosage regulates cell fate divergence during distinct phases of PF network morphogenesis.

Introduction

The cardiac conduction system (CCS) is essential to initiate and propagate electrical activity throughout the entire heart [1,2]. Efficient heartbeats require perfect coordination between conduction and contraction driven by specialized conductive and contractile cardiomyocytes, respectively. In the ventricles, the terminal conduction system consists of Purkinje fiber cells (PFs) characterized by fast conduction properties necessary to activate the ventricular myocardium from the apex to the base and ensure the efficient expulsion of the blood. PFs are organized in a complex network of fascicles forming ellipsoidal structures[3]. Despite their functional importance and identification of PFs as a major trigger of ventricular arrhythmias[4], it is still unclear how the complex PF network forms during ventricular morphogenesis[5-8].

During ventricular development, trabecular myocardium expressing the gap junction protein Connexin40 (Cx40; Gja5) constitutes the primary fast-conducting pathway[9]. An important finding came from clonal studies in chick, showing that PFs shared a common myogenic origin with contractile cardiomyocytes of the working myocardium[10]. More recently, using genetic tracing and retrospective clonal analysis, it has been demonstrated that murine ventricular trabeculae contain PF progenitor cells. Moreover, the ventricular conduction system (VCS) displays a biphasic development involving lineage restriction to a conductive phenotype followed by limited proliferative outgrowth. Lineage restriction between trabecular cardiomyocytes and PFs is largely complete by E16.5[11, 12]. However, key questions concern when and how trabecular cells diverge towards the conductive or contractile lineage during development. To identify the timing of lineage segregation of contractile and conductive cardiomyocytes within the trabecular progenitor cell population, an *in vivo* temporal clonal analysis is required. Clonal analysis, consisting of the genetic labeling of an individual cell at a defined developmental stage and studying its progeny at a later stage, is a powerful approach to assess cell fate and cell behavior within a heterogeneous progenitor population.

The transcription factor NKX2-5 is highly conserved across evolution in vertebrates and one of the earliest markers of the developing heart[13]. In the human population, *NKX2-5* mutations

represent around 4% of congenital heart diseases (CHDs) with a high prevalence of conduction disturbances and arrhythmias[14]. Many studies have highlighted the importance of Nkx2-5 for the formation and the maintenance of the conduction system[15]. Conduction defects observed in *Nkx2-5* heterozygous mice have been correlated with an hypoplasia of the VCS associated with a reduced PF network lacking ellipsoidal structures[16, 17]. Moreover, patients carrying *NKX2-5* mutations display noncompaction cardiomyopathy[18] and *Nkx2-5* expression is required during trabecular development to prevent hypertrabeculation[19, 20]. By performing temporal clonal analysis of cardiac progenitors, we have uncovered distinct phases of PF network morphogenesis: an initial bipotent-progenitor-dependent scaffolding phase and a later conductive progenitor recruitment phase. Extending our analysis to *Nkx2-5* heterozygous mutant mice we have deciphered the temporal requirement of Nkx2-5 during the segregation of trabecular cells towards the conductive lineage and gained mechanistic insight into the etiology of PF hypoplasia.

Results

Nkx2.5 haploinsufficiency specifically affects cell fate choice into conductive but not trabecular lineage

To establish the lineage contribution of trabecular cells to the VCS during ventricular development, we performed genetic fate mapping of *Cx40*+ cells. *Cx40* expression is first observed in atrial and ventricular cardiomyocytes at embryonic day (E) E9.5[21]. Between E10.5 and E14.5, *Cx40* is strongly expressed in ventricular trabeculae and restricted to conductive cells of the VCS at birth[12]. *Cx40-CreERT2*[22] mice were crossed with *Rosa26-YFP* conditional lineage reporter mice and Cre recombination was activated by tamoxifen injections at different embryonic days, prior to analysis at postnatal day 7 (P7; Supplementary Fig. 1). Cells expressing *Cx40* in the embryonic (E10.5) and fetal (E14.5) heart actively contribute to both the left ventricular free wall and VCS. In contrast, after tamoxifen injection at P1, *Cx40*-derived cell numbers are reduced and restricted to the VCS.

Consistent with previous reports, this shows the progressive fate restriction of *Cx40*-positive trabecular cells to the VCS lineage[23].

In order to investigate the mechanisms underlying PF hypolasia in *Nkx2-5* haploinsufficient hearts, we performed similar inducible genetic tracing in *Nkx2-5* heterozygous mice. *Cx40*-trabecular cells were labelled at E14.5 and their contribution to the VCS assayed by Cx40-RFP (PF) and YFP (Trabecular-derived) expression at P7 (Fig. 1a-c). We observed that the total number of trabecular-derived cells is similar in *Nkx2-5*$^{+/-}$ and control hearts (Fig. 1e, Supplementary Fig. 1). However, the contribution of trabecular cells to the VCS is highly reduced with only 6% of YFP+ cells expressing RFP in *Nkx2-5*$^{+/-}$ hearts compared to 20% in the wild-type situation (Fig. 1f), consistent with a reduced number of PFs is in *Nkx2-5*$^{+/-}$ hearts (Fig. 1d). Fetal *Cx40*+ trabecular cells thus predominantly contribute to working myocardium in *Nkx2-5* haploinsufficient hearts, demonstrating that the acquisition of PF cell fate is selectively and severely affected (Fig. 1g).

Temporal clonal analysis of single Cx40+ cells defines two phases of segregation of trabecular cells to the conductive lineage

To determine whether trabecular cells exhibit bipotency at the cellular level, and when the segregation of conductive and contractile cell fate choice occurs, we performed clonal analysis using the multicolor Rosa26-Confetti reporter mouse line at different timepoints of development. We used *Cx40-CreERT2* mice to genetically mark trabecular cardiomyocytes with a low dose of 4OH-tamoxifen. This generates hearts containing distinct clusters derived from different individual cells stochastically labelled by one of the four colors on recombination of the confetti cassette (Fig. 2a,b; Supplementary Fig. 2a). The absence of clusters containing multicolor cells is a strong argument that cells within each cluster can be considered to be clonally related[24]. The frequency of clusters observed in control and *Nkx2-5*$^{+/-}$ hearts was identical, indicating that the probability of generating *Cx40*-derived clones is not affected by reduced levels of *Nkx2-5* (Table 1). Immunofluorescence against Contactin 2 (CNTN2), identifying mature PF cells, was used to distinguish three types of clusters. Conductive clones are

composed of 100% CNTN2-positive cells and are likely to result from labeling of a lineage restricted conductive precursor cell. Clones in which only a sub-population of labelled cells are CNTN-2-positive were classified as mixed and originate from a bipotent progenitor. Finally, non-conductive clones with no CNTN2-positive cells originate from a recombination in a working cardiomyocyte precursor cell (Fig. 2c).

Clonal labeling of *Cx40+* cells at E9.5 produced a collection of conductive, mixed and non-conductive clones, indicating the heterogeneity of Cx40+ progenitors present at this timepoint. Unexpectedly, 39% of these unicolor clones contained exclusively CNTN2 positive conductive cells, indicating that a third of Cx40+ trabecular cells are already committed to a PF fate at E9.5 (Fig. 2d). A similar percentage was observed in both *Nkx2-5*$^{+/-}$ and control littermates, indicating that *Nkx2-5* haploinsufficiency does not impact on early commitment to the PF lineage (Fig. 2e). Induced labeling at later stages of development demonstrates the progressive loss of bipotency of Cx40+ trabecular cells, as shown by a reduction in the number of mixed clones over time (Fig. 2f). Conversely the proportion of conductive clones increases with time, consistent with progressive restriction of fate and *Cx40* expression to the conductive lineage. Independent of their date of birth or whether they are generated in wildtype or *Nkx2-5* heterozygous mutant hearts, conductive clones always contain a small number of cells (<20), consistent with loss of proliferation on segregation to the conductive lineage (Supplementary Fig. 3). This implies that the development of the VCS occurs by progressive recruitment of committed progenitors as proposed by the ingrowth model[5, 25]. Tracing the kinetics of apparition of the conductive clones defines an early phase of slow recruitment until E14.5 followed by a phase of rapid recruitment at late fetal stages (Fig. 2f). In *Nkx2-5*$^{+/-}$ mice, the progressive recruitment of committed progenitors to the VCS is severely affected, preventing their differentiation into conductive cells, particularly during the phase of rapid recruitment as shown by the high proportion of non-conductive clones labeled at E18.5. In contrast to the wildtype situation, mixed clones are observed in *Nkx2-5*$^{+/-}$ hearts after labelling at E18.5, revealing that Cx40+ bipotent progenitor cells persist abnormally in *Nkx2-5*$^{+/-}$ hearts at birth. Together these results indicate a

requirement of maximal levels of *Nkx2-5* for progressive recruitment to the VCS during fetal development.

To study if the hypoplasia of the PF network in Nkx2-5 heterozygotes mice results from a disturbance in the timing of these two phases of recruitment, we performed temporal genetic fate mapping and quantified the relative proportion of trabecular cells giving rise to PF. A similar proportion of trabecular cells contributing to PF at E9.5 and E14.5 was observed in control and *Nkx2-5*$^{+/-}$ hearts, reinforcing the idea that the kinetics of the early phase of recruitment is unchanged by a reduced level of Nkx2-5 (Fig. 2g and Supplementary Fig. 4a-c). In contrast, when labelled at E18.5, trabecular cells contribute to a larger proportion of the *Nkx2-5*$^{+/-}$ PF (54%) at P7 compared to control hearts (42%) (Fig. 2g). This supports the absence of rapid recruitment of new conductive cells in *Nkx2-5*$^{+/-}$ hearts at late fetal stages. Moreover, this shows that at E9.5, the onset of trabeculation, labeled trabecular cells only participate to a small proportion of PF (10%) while this proportion increases on labelling at E14.5 (35%). Cx40+ trabecular cells thus do not represent the totality of VCS progenitors and early Cx40-negative progenitor cells contribute to the growth of the PF network.

Conductive cells of the PF lineage are present at the linear heart tube stage and define distinct populations of progenitors.

To study the contribution of earlier progenitors to the VCS, the smooth muscle actin *SMA-CreERT2* mouse line was used to label differentiated cardiomyocytes from the cardiac crescent stages (E7.5), prior to the onset of *Cx40* expression[26]. Genetic tracing using Rosa-YFP reporter mice shows that early cardiomyocytes contribute to the PF in equivalent proportions in control and *Nkx2-5* heterozygous mutant embryos (Supplementary Fig. 4d). Then, we examined the cellular behavior of early labelled cardiomyocyte clones during segregation of conductive and contractile fates using *Rosa-confetti* mice and a low dose of 4OH-tamoxifen (Fig 3a, b). As SMA is expressed in all cardiomyocytes, we observed a large number of non-conductive clones in 3-weeks-old whole hearts

from control and *Nkx2-5*$^{+/-}$ mice (Supplementary Fig. 2b) and focused our study on conductive and mixed clones. Consistent with early segregation of cardiac progenitors towards the PF lineage, conductive clones were observed after labeling at both E8.5 and E7.5 (Supplementary Fig. 5). Such conductive clones were observed in both control and *Nkx2-5* heterozygous hearts (Fig. 3c). Together, these results demonstrate that the early segregation of the PF lineage within SMA-positive cells starts at or before the onset of heart tube formation, before trabeculation begins. Moreover, consistent with our observations using the *Cx40-CreERT2* line, this early segregation is unaffected by *Nkx2-5* haploinsufficiency[27].

Tracing the relative proportion of mixed clones induced at different embryonic days E7.75, E8.5, E9.5 and E10.5, revealed a similar decrease of bipotent progenitors with time both in control and *Nkx2-5*$^{+/-}$ hearts (Fig. 3d). This illustrates the progressive lineage restriction of cardiac progenitor cells to working or conductive fate during the early recruitment phase. However, a higher number of mixed clones were observed in *Nkx2-5* heterozygous hearts at each time point, suggesting that a larger number of SMA-positive cardiac progenitors fail to segregate into the conductive lineage.

A detailed analysis of the clone size distribution induced by SMA-CreERT2 at E8.5 revealed that mixed clones are heterogeneous in size and that large mixed clones (>80) are absent in *Nkx2-5*$^{+/-}$ hearts (Fig. 3e). In control hearts, the presence of large mixed clones is consistent with the high proliferative capacity of bipotent progenitors while the conductive compartment remains small and of comparable size between control and *Nkx2-5*$^{+/-}$ hearts (Supplementary Fig. 3, Table 1). These data show that a reduced level of *Nkx2-5* expression affects the cellular behavior of bipotent progenitors originating from early differentiating cardiomyocytes. Two hypotheses may explain this discrepancy: either a reduced proliferative capacity of these bipotent progenitors or an absence of recruitment of proliferative progenitors to the VCS. Together, these data suggest that the early (E8.5) heart contains a population of progenitor cells that do not express Cx40 and will later contribute to trabeculae and the VCS. The subsequent development of this population of progenitor cells is particularly affected by a reduced level of Nkx2-5 impacting their later contribution to the PF network.

Nkx2-5 haploinsufficient hearts present a hypoplastic PF network due to impaired recruitment of early cardiac progenitors

To further investigate the mechanism underlying the lack of recruitment of cells derived from early progenitors to the VCS, we studied the contribution of all cardiac progenitors by mosaic tracing analysis using *Mesp1-Cre* and *Rosa-confetti* mice (Fig. 4a, b). *Mesp1* is expressed during a short time window during gastrulation, and the *Mesp1-Cre* allele induces spatio-temporally restricted Cre activation in mesodermal progenitors, generating clones born between E6.5 and E7.5[24]. The overall distribution of *Mesp1-Cre* activated confetti (RFP, YFP, CFP, GFP) clusters is indistinguishable in hearts from control and *Nkx2-5*$^{+/-}$ mice (Fig. 4c; Supplementary Fig. 2c). However, while in control hearts, the PF network made by multiple fascicles forming ellipsoidal structures is dense and complex, in *Nkx2-5*$^{+/-}$ hearts, the network is hypoplastic with less ellipses and thinner fascicles (Fig. 4c). However, each fascicle is composed of multicolor *Mesp1* lineage labelled cells in both wildtype and *Nkx2-5*$^{+/-}$ hearts (Fig. 4c). *Mesp1*-labeled cells within the VCS were highlighted to show the polyclonal development of the PF network composed of a tangle of multicolor fascicles supporting the ingrowth model (Fig. 4d). Closer examination of these images showed that the complex PF network is composed of both small and large monochromatic clusters in control hearts while only small clusters contribute to the hypoplastic network in *Nkx2-5*$^{+/-}$ hearts. The presence of large monochromatic clusters might reflect a clonal dominance and is consistent with the relative small number of progenitors giving rise to the myocardium in mice (~230) or zebrafish (~8) hearts [28, 29]. The absence of large monochromatic clusters is consistent with the lack of recruitment of PFs from a pool of proliferative progenitors to the PF network in *Nkx2-5* haploinsufficient mice.

Next, we quantified the contribution of *Mesp1*-derived cells to the VCS on sections and could not detect a difference in the overall proportion of confetti-labeled cells between control and Nkx2-5 heterozygous mutant hearts (Supplementary Fig. 4f, g). Interestingly, this proportion is quite similar

to the contribution of Cx40-labelled trabecular cells at E14.5 suggesting that PF derive entirely from these cells and not from another source of progenitors. However, comparing the ratio of the four possible single-color clusters in the two cases, we observed a majority of RFP and YFP labeled cells in control hearts, while the proportion is almost equally distributed for RFP, YFP and CFP in the mutant (Supplementary Fig. 4h). A lower proportion of GFP+ cells in both control and mutant hearts is explained by its nuclear localization which make these cells invisible when the nucleus is absent on the section and the fact that this color is usually less represented than the others on recombination of the Confetti cassette[30]. However, control and *Nkx2-5*$^{+/-}$ hearts show similar distribution of individual confetti colors in left ventricular myocardium, consistent with the whole-mount analysis (Supplementary Fig. 4i). In control hearts, the distribution of the proportion of each color from individual hearts in PF versus left ventricular myocardium follows a linear regression with a correlation coefficient close to 1 (r^2=0,96±0,03) demonstrating a proportional growth of these two compartments (Fig. 4g). These data fit well with recent evidence for the existence of a hybrid zone, showing that the ventricular myocardium grows by proliferation of compact myocardium invading up to the subendocardial zone[31]. In contrast, this distribution of each color to PF and working myocardial clusters is not correlated in *Nkx2-5*$^{+/-}$ hearts (r^2=0,32±0,27) suggesting that the PF network grows independently from the working myocardium or with a limited contribution of the hybrid zone to the PF (Fig. 4g). These discrepancies may result from differences in the cell behavior of progenitor cells, such as their rate of proliferative. Indeed, inducible lineage tracing analysis of Mesp1 progenitors has identified a more proliferative subpopulation of cardiac progenitors induced at E6.75[28]. These results suggest that while PFs arise globally from the same progenitors (Mesp1 and SMA), the network is formed by different subpopulations of progenitors. Together, these data reinforce and extend our previous hypothesis suggesting that the PF network develops in two phases[17]. During the early phase of recruitment, committed conductive cells arise from poorly proliferative progenitor cells and give rise to small clusters that provide a scaffold for a polyclonal PF network, then at late fetal stages, rapid recruitment of newly-committed cells participates in the building of a more complex network

indicated by large monochromatic clusters (Fig. 5). In *Nkx2-5*$^{+/-}$ hearts, this last recruitment step fails and the PF network remains in its early state.

Nkx2-5 haploinsufficiency disturbs the morphogenesis of PF network during embryonic development but not its maintenance after birth.

To investigate whether PF hypoplasia in Nkx2-5 heterozygous mice may also result from a defect in maintenance of a conduction phenotype after birth, we carried out a genetic tracing analysis of *Cx40*-derived trabecular cells at birth (Fig. 6a). After E18.5 labeling, the majority of YFP+ cells were conductive in control hearts, while in *Nkx2-5*$^{+/-}$ hearts a large number of YFP+ cells were CNTN-2 negative (Fig. 6b, Supplementary Fig. 4c). High magnification of control hearts revealed a well-organized network of YFP+/CNTN-2+ PFs forming ellipsoidal structures while YFP+/CNTN-2- cells in *Nkx2-5* heterozygous hearts exhibited a parallel alignment, and presented a rectangular cell shape, which is a typical morphology of working cardiomyocytes (Fig. 6b") in comparison with the thin and elongated shape of PF (Fig. 6a" and Supplementary Fig. 5). These results strongly suggest that *Nkx2-5* haploinsufficient *Cx40* positive cells are maintained at birth as shown by the clonal analysis but fail to differentiate into conductive cells. In order to study the temporal effect of *Nkx2-5* deletion, we performed genetic tracing of Cx40+ cells in mice in which one allele of *Nkx2-5* was deleted upon tamoxifen injection at E18.5 (Fig. 5c). In *Nkx2-5-floxed/+* mice, YFP+ cells displayed a comparable cell shape and organization to that observed in control mice, indicating that reduction of Nkx2-5 expression after birth does not affect the differentiation of Cx40+ cells and the formation of the PF network is maintained. These data demonstrate that the morphogenesis of the PF network occurs before birth and requires a maximal level of *Nkx2-5* expression in embryonic cardiomyocytes.

Discussion

While genetic lineage tracing has proven to be very useful to study the fate of specific progenitors such as trabecular cells that give rise to both PFs and working myocardium[12], distinct cellular behaviors within this progenitor cell population have not been analyzed to date. In this study, we exploit the power of mosaic genetic tracing and temporal clonal analyses using inducible Cre lines to dissect the sequential events occurring during the development of the PF network. We demonstrate, for the first time, that *Cx40*+ trabeculae constitute a heterogeneous pool of progenitors that includes cells committed to the conductive lineage as early as E9.5. Moreover, a subpopulation of early cardiac progenitors is already fated to the PF lineage at the onset of the heart tube formation (E7.75), prior to *Cx40* expression. This unexpected early segregation of cardiac progenitor cells to a PF fate is unaffected by *Nkx2-5* haploinsufficiency. Recently, it has been shown that central components of the cardiac conduction system are already committed before heart tube formation[27, 32] and are derived from early cardiomyocytes expressing Tbx3[33]. However, it was unknown whether cells of the murine PF network, that grows at least in part through later recruitment to a PF fate, were also committed at such early stages. Our data demonstrate that peripheral VCS precursors of the PF network, like central VCS components, emerge from populations of cardiac progenitor cells that are specified but remain electrically inactive during the initial stages of heart tube development, as has been shown for pacemaker progenitor cells in avian embryos[32]. Inductive cues that govern the VCS lineage fate choice are poorly understood. However, in *Nkx2-5* null embryos, the pool of conductive progenitors delineated by *Mink-LacZ*+ is absent[34] and deletion of *Nkx2-5* in embryonic trabeculae at E10.5 abolishes the formation of the PF network[20].

The presence of mixed conductive and working myocardial clones in our experiments shows that growth of the definitive peripheral VCS requires the progressive addition of cells from bipotent progenitor cells. Our lineage tracing analysis supports a model by which lineage restriction to the conductive fate is progressive during heart morphogenesis [35]. While trabecular identity is conserved

in *Nkx2-5*$^{+/-}$ cardiomyocytes, they progressively lose their capacity to differentiation into a PF fate. In wildtype hearts, bipotent cells with high proliferative capacity make a massive lineage contribution to the PF network before birth. Such progenitors have been described in the compact zone of the embryonic heart and contribute to ventricular myocardial expansion through the invasion of cells in the compact zone towards the inner surface of the ventricle during development [31]. Our data suggest that these progenitor cells are more affected by *Nkx2-5* haploinsufficiency than early differentiating trabeculae. In contrast to previous data suggesting that *Nkx2-5* downregulates trabecular proliferation[19], we do not observe an increase of clone size in *Nkx2-5* heterozygote mice. Our results highlight the fact that Nkx2-5 plays a major role in the differentiation of trabecular cells towards a PF phenotype but not in their proliferation. This is consistent with previous studies suggesting that elevated levels of *Nkx2-5* expression defines a population of cardiomyocytes actively differentiating into a conductive phenotype and that precise temporal regulation of Nkx2-5 levels may be necessary for normal differentiation of Purkinje fiber cells[15,36,37]. Conversely, reduced Nkx2-5 levels may play a role in the maintenance of proliferative status of progenitors. In accordance with this hypothesis, single-cell RNA-sequencing has demonstrated that *Nkx2-5*$^{+/-}$ mice exhibit higher numbers of immature cardiomyocytes in the left ventricle compared to control mice, especially at E14.5[38]. These data strongly suggest that PF differentiation is impaired in Nkx2-5 haploinsufficient cardiomyocytes that instead maintain a progenitor-like phenotype.

This study is the first to address clonal contributions to the developing PF network. The conditional deletion of one *Nkx2-5* allele at birth shows no effect on the differentiation of Cx40+ cells or morphogenesis of the PF network. Thus, our experiments demonstrate that a high level of Nkx2-5 is required during embryonic stages for the formation of the VCS rather than playing a role in maintenance of the PF network. Our temporal clonal analysis of trabecular cells demonstrates that the PF network grows principally by gradual addition of newly committed cells rather than by proliferation of conductive precursors. Indeed, the size of conductive clones labelled during

embryogenesis is smaller than that of non-conductive clones, confirming that segregation into conductive fate is associated with a loss of proliferative capacity[12]. The size of non-conductive clones generated after E14.5 labelling, is similar to that of conductive clones, demonstrating the decrease of the proliferative capacities of cardiomyocytes at perinatal stages, as previously demonstrated[39]. As expected for a tissue with a low proliferative index[40], the stochastic labeling of conductive cells generated a mosaic pattern forming a polyclonal network with conductive cells sparsely distributed within the ellipses. The kinetics of apparition of conductive clones is biphasic with a first phase of recruitment from heart tube stage until E14.5 during which the commitment of new conductive cells is slow and similar between *Nkx2-5*$^{+/-}$ and control mice. Maximal levels of Nkx2-5 is dispensable for the early phase of PF network formation including early commitment and initial recruitment of conductive cells during trabecular development. We cannot exclude the possibility that other transcription factors are able to compensate the lack of Nkx2-5 during the early stages of development. Finally, these data suggest that the residual PF network present in *Nkx2-5*$^{+/-}$ hearts represents the persistence of this early network. This structure defines an embryonic scaffold for the later PF network as, at late fetal stages, the number of new committed PF increased rapidly and are added to the early scaffold to form a complex PF network through a mechanism dependent on maximal Nkx2-5 expression levels. The exact molecular mechanisms leading to the formation of this network need further investigation. However, the resemblance of PF hypoplasia phenotype in IRX3 and ETV1 mutants with Nkx2.5 heterozygotes suggests a cooperative effect between these transcription factors[41, 42]. Interestingly, the rapid recruitment of PF cells occurs during trabecular compaction which is also altered in *Nkx2-5* mutant hearts and affected in human patients presenting non-compaction cardiomyopathies, often associated with arrhythmias[20, 43].

In conclusion, our temporal clonal analysis of the mammalian VCS using the confetti system has uncovered sequential steps in the peripheral VCS development and the etiology of PF hypoplasia observed in adult *Nkx2-5* heterozygous mice. Finally, our observation that progenitor-like cells persist

in the mature *Nkx2-5*$^{+/-}$ heart is an important finding for the design of future therapeutic strategies. As *Nkx2-5* mutations are highly frequent and represent 4% of CHD, deciphering cues that may drive the fate of these cells into the conductive lineage would represent a valuable strategy to treat conductive disorders and ventricular arrhythmias.

online Methods

Animals and injections

The *Cx40-CreERT2*[22], *Sma-CreERT2*[44], Mesp1-cre[45], *R26R-YFP*[46], *R26R-Confetti* [30], *Nkx2-5-lacZ*[47] and *Nkx2-5-floxed*[48] mouse lines have been previously reported. For genetic tracing analysis, *Cx40-CreERT2* males were crossed with *R26R-YFP* females and tamoxifen was injected intraperitoneally to pregnant females (200µl) for one or two consecutive days or to newborn in a single injection (10µl). Tamoxifen (T5648, Sigma) was dissolved at the concentration of 20mg/ml in ethanol/sunflower oil (10:90). After tamoxifen treatment to pregnant females, newborn mice were recovered after caesarian and gave for adoption to CD1 females. For prospective clonal analysis, *Sma-CreERT2* or *Cx40-CreERT2* males were crossed with *R26-Confetti* females and low doses of 4-Hydroxytamoxifen (4-OHT H6278, Sigma) was injected intraperitoneally to pregnant females in a single injection. 4-OHT was dissolved at the concentration of 10mg/ml in ethanol/ Cremophor® EL (Sigma) solution (50:50). Before injection, 4-OHT was diluted in 1X PBS and 200 µL of this solution was injected intraperitoneally into pregnant females.

Antibodies and immunofluorescence

Antibodies used in this study are specific to Nkx2-5 (Sc8697 Santa-Cruz, Dallas, TX, USA), GFP (AbD Serotec, Bio-Rad, Hercules, CA, USA), PECAM-1 (MEC13.3-BD Pharmingen) and Contactin-2 (AF1714 R&D Systems, Minneapolis, MN, USA). For whole-mount immunofluorescence, hearts were dissected and fixed in 2% paraformaldehyde overnight at 4°C, washed in PBS, permeabilized in PBS 1X/0.5% Triton X100 for 1 h and incubated for 3 h in saturation buffer (PBS 1X; 3% BSA; 0.1% Triton X100). The primary antibodies were incubated in saturation buffer for two days at 4 °C. Secondary antibodies coupled to fluorescent molecules were incubated in saturation buffer and after washes, hearts were observed under a Zeiss Lumar stereomicroscope V12 or Zeiss LSM780 confocal microscope. For immunofluorescence on cryostat sections, hearts were permeabilized for 20 minutes (PBS 1X / 0.2% Triton X100) and blocked for 1 hour (PBS 1X / 3% Bovine Serum Albumin / 0.1% TritonX100/ 0.05%

Saponin). The primary antibodies were incubated in blocking buffer for overnight at 4°C. Secondary antibodies coupled to fluorescent molecules were incubated in blocking buffer for 1 hour. After washes hearts were observed under a Zeiss Z1 Apotome microscope.

Clonal analysis

4-OHT injections were performed at different time points of development to induce rare recombination events, generating well-separated clones. At 3 weeks, hearts were dissected and pinned on petri dish to expose the inner side of the left ventricle and fixed in 2% Paraformaldehyde overnight at 4°C and washed in PBS 1X. They were permeabilized for 1 hour (PBS 1X / 0.5% Triton X100) and blocked for 3 hours (PBS 1X / 3% Bovine Serum Albumin / 0.1% Triton X100). The primary anti-Contactin-2 antibody was incubated in blocking buffer for 48 hours at 4°C. Secondary antibody coupled to fluorescent molecule was incubated in blocking buffer for 48 hours and after washes, hearts were observed under a Zeiss LSM780 confocal microscope. Individual clusters were analyzed on virtual sections using the software Volocity. A single clone corresponds to a cluster composed of cells of only one color (RFP, GFP, YFP, or CFP) that are distributed in consecutive sections.

Acknowledgments

We are grateful to Sabrina Lefèvre-Beyer and Caroline Giessner for their involvement in the initiation and technical contributions to this project. We thank N. Bertrand, C. Cortes and F. Lescroart for critical discussions and reading of the manuscript. We acknowledge the France-BioImaging/PICsL infrastructure (ANR-10-INSB-04-01).

This work was supported by the CNRS, the Association Française contre les Myopathies (AFM) (LM) and the Fondation pour la Recherche Médicale (FRM) (RK). CC was the recipient of GRRC/SFC PhD and AFM postdoc fellowships.

Author Contributions

C.C., L.M. conceived the project and designed the experiments; C.C. performed most of the temporal clonal experiments; C.C. and L.M. performed genetic tracing experiments; C.C. performed the statistical analysis. R.G.K. and L.M. provided funding; R.G.K. reviewed and edited the manuscript; C.C. and L.M. wrote the manuscript.

Competing Interests statement

None.

References

1. Dobrzynski, H. *et al.* Structure, function and clinical relevance of the cardiac conduction system, including the atrioventricular ring and outflow tract tissues. *Pharmacol Ther* **139**, 260-288 (2013).
2. Anderson, R.H. & Ho, S.Y. The morphology of the cardiac conduction system. *Novartis Found Symp* **250**, 6-17; discussion 18-24, 276-279 (2003).
3. Miquerol, L. *et al.* Architectural and functional asymmetry of the His-Purkinje system of the murine heart. *Cardiovasc Res* **63**, 77-86 (2004).
4. Haissaguerre, M. *et al.* Role of Purkinje conducting system in triggering of idiopathic ventricular fibrillation. *Lancet* **359**, 677-678 (2002).
5. Mikawa, T. & Hurtado, R. Development of the cardiac conduction system. *Semin Cell Dev Biol* **18**, 90-100 (2007).
6. Miquerol, L., Beyer, S. & Kelly, R.G. Establishment of the mouse ventricular conduction system. *Cardiovasc Res* **91**, 232-242 (2011).
7. Moorman, A.F. & Christoffels, V.M. Development of the cardiac conduction system: a matter of chamber development. *Novartis Found Symp* **250**, 25-34; discussion 34-43, 276-279 (2003).
8. van Eif, V.W.W., Devalla, H.D., Boink, G.J.J. & Christoffels, V.M. Transcriptional regulation of the cardiac conduction system. *Nat Rev Cardiol* **15**, 617-630 (2018).
9. Sedmera, D. *et al.* Spatiotemporal pattern of commitment to slowed proliferation in the embryonic mouse heart indicates progressive differentiation of the cardiac conduction system. *Anat Rec A Discov Mol Cell Evol Biol* **274**, 773-777 (2003).
10. Cheng, G. *et al.* Development of the cardiac conduction system involves recruitment within a multipotent cardiomyogenic lineage. *Development* **126**, 5041-5049 (1999).

11. Miquerol, L. *et al.* Resolving cell lineage contributions to the ventricular conduction system with a Cx40-GFP allele: a dual contribution of the first and second heart fields. *Dev Dyn* **242**, 665-677 (2013).

12. Miquerol, L. *et al.* Biphasic development of the mammalian ventricular conduction system. *Circ Res* **107**, 153-161 (2010).

13. Harvey, R.P. *et al.* Homeodomain factor Nkx2-5 in heart development and disease. *Cold Spring Harb Symp Quant Biol* **67**, 107-114 (2002).

14. Ellesoe, S.G. *et al.* Familial Atrial Septal Defect and Sudden Cardiac Death: Identification of a Novel NKX2-5 Mutation and a Review of the Literature. *Congenit Heart Dis* **11**, 283-290 (2016).

15. Moskowitz, I.P. *et al.* A molecular pathway including Id2, Tbx5, and Nkx2-5 required for cardiac conduction system development. *Cell* **129**, 1365-1376 (2007).

16. Jay, P.Y. *et al.* Nkx2-5 mutation causes anatomic hypoplasia of the cardiac conduction system. *J Clin Invest* **113**, 1130-1137 (2004).

17. Meysen, S. *et al.* Nkx2.5 cell-autonomous gene function is required for the postnatal formation of the peripheral ventricular conduction system. *Dev Biol* **303**, 740-753 (2007).

18. Ashraf, H. *et al.* A mouse model of human congenital heart disease: high incidence of diverse cardiac anomalies and ventricular noncompaction produced by heterozygous Nkx2-5 homeodomain missense mutation. *Circ Cardiovasc Genet* **7**, 423-433 (2014).

19. Pashmforoush, M. *et al.* Nkx2-5 pathways and congenital heart disease; loss of ventricular myocyte lineage specification leads to progressive cardiomyopathy and complete heart block. *Cell* **117**, 373-386 (2004).

20. Choquet, C. *et al.* Deletion of Nkx2-5 in trabecular myocardium reveals the developmental origins of pathological heterogeneity associated with ventricular non-compaction cardiomyopathy. *PLoS Genet* **14**, e1007502 (2018).

21. Delorme, B. *et al.* Expression pattern of connexin gene products at the early developmental stages of the mouse cardiovascular system. *Circ Res* **81**, 423-437 (1997).

22. Beyer, S., Kelly, R.G. & Miquerol, L. Inducible Cx40-Cre expression in the cardiac conduction system and arterial endothelial cells. *Genesis* **49**, 83-91 (2011).

23. Li, Y. *et al.* Genetic targeting of Purkinje fibres by Sema3a-CreERT2. *Sci Rep* **8**, 2382 (2018).

24. Lescroart, F. *et al.* Early lineage restriction in temporally distinct populations of Mesp1 progenitors during mammalian heart development. *Nature cell biology* **16**, 829-840 (2014).

25. Mikawa, T. *et al.* Induction and patterning of the Purkinje fibre network. *Novartis Found Symp* **250**, 142-153; discussion 153-146, 276-149 (2003).

26. Armstrong, J.J., Larina, I.V., Dickinson, M.E., Zimmer, W.E. & Hirschi, K.K. Characterization of bacterial artificial chromosome transgenic mice expressing mCherry fluorescent protein substituted for the murine smooth muscle alpha-actin gene. *Genesis* **48**, 457-463 (2010).

27. Choquet, C., Marcadet, L., Beyer, S., Kelly, R. & Miquerol, L. Segregation of Central Ventricular Conduction System Lineages in Early SMA+ Cardiomyocytes Occurs Prior to Heart Tube Formation. *J. Cardiovasc. Dev. Dis.* **3**, 2 (2016).

28. Chabab, S. *et al.* Uncovering the Number and Clonal Dynamics of Mesp1 Progenitors during Heart Morphogenesis. *Cell Rep* **14**, 1-10 (2016).

29. Gupta, V. & Poss, K.D. Clonally dominant cardiomyocytes direct heart morphogenesis. *Nature* **484**, 479-484 (2012).

30. Snippert, H.J. *et al.* Intestinal crypt homeostasis results from neutral competition between symmetrically dividing Lgr5 stem cells. *Cell* **143**, 134-144 (2010).

31. Tian, X. *et al.* Identification of a hybrid myocardial zone in the mammalian heart after birth. *Nat Commun* **8**, 87 (2017).

32. Bressan, M., Liu, G. & Mikawa, T. Early mesodermal cues assign avian cardiac pacemaker fate potential in a tertiary heart field. *Science* **340**, 744-748 (2013).

33. Mohan, R.A. *et al.* Embryonic Tbx3+ cardiomyocytes form the mature cardiac conduction system by progressive fate restriction. *Development* (2018).

34. Jay, P.Y. *et al.* Function follows form: cardiac conduction system defects in Nkx2-5 mutation. *Anat Rec* **280A**, 966-972 (2004).

35. van Eif, V.W.W., Stefanovic, S., Mohan, R.A. & Christoffels, V.M. Gradual differentiation and confinement of the cardiac conduction system as indicated by marker gene expression. *Biochim Biophys Acta Mol Cell Res* (2019).

36. Harris, B.S. *et al.* Differentiation of cardiac Purkinje fibers requires precise spatiotemporal regulation of Nkx2-5 expression. *Dev Dyn* **235**, 38-49 (2006).

37. Thomas, P.S. *et al.* Elevated expression of Nkx-2.5 in developing myocardial conduction cells. *Anat Rec* **263**, 307-313 (2001).

38. DeLaughter, D.M. *et al.* Single-Cell Resolution of Temporal Gene Expression during Heart Development. *Dev Cell* **39**, 480-490 (2016).

39. Sereti, K.I. *et al.* Analysis of cardiomyocyte clonal expansion during mouse heart development and injury. *Nat Commun* **9**, 754 (2018).

40. Chappell, J. *et al.* Extensive Proliferation of a Subset of Differentiated, yet Plastic, Medial Vascular Smooth Muscle Cells Contributes to Neointimal Formation in Mouse Injury and Atherosclerosis Models. *Circ Res* **119**, 1313-1323 (2016).

41. Kim, K.H. *et al.* Irx3 is required for postnatal maturation of the mouse ventricular conduction system. *Sci Rep* **6**, 19197 (2016).

42. Shekhar, A. *et al.* Transcription factor ETV1 is essential for rapid conduction in the heart. *J Clin Invest* **126**, 4444-4459 (2016).

43. Costa, M.W. *et al.* Functional characterization of a novel mutation in NKX2-5 associated with congenital heart disease and adult-onset cardiomyopathy. *Circ Cardiovasc Genet* **6**, 238-247 (2013).

44. Wendling, O., Bornert, J.M., Chambon, P. & Metzger, D. Efficient temporally-controlled targeted mutagenesis in smooth muscle cells of the adult mouse. *Genesis* **47**, 14-18 (2009).

45. Saga, Y. *et al.* MesP1 is expressed in the heart precursor cells and required for the formation of a single heart tube. *Development* **126**, 3437-3447 (1999).

46. Srinivas, S. *et al.* Cre reporter strains produced by targeted insertion of EYFP and ECFP into the ROSA26 locus. *BMC Dev Biol* **1**, 4 (2001).

47. Tanaka, M., Chen, Z., Bartunkova, S., Yamasaki, N. & Izumo, S. The cardiac homeobox gene Csx/Nkx2.5 lies genetically upstream of multiple genes essential for heart development. *Development* **126**, 1269-1280 (1999).

48. Furtado, M.B. *et al.* A novel conditional mouse model for Nkx2-5 reveals transcriptional regulation of cardiac ion channels. *Differentiation* **91**, 29-41 (2016).

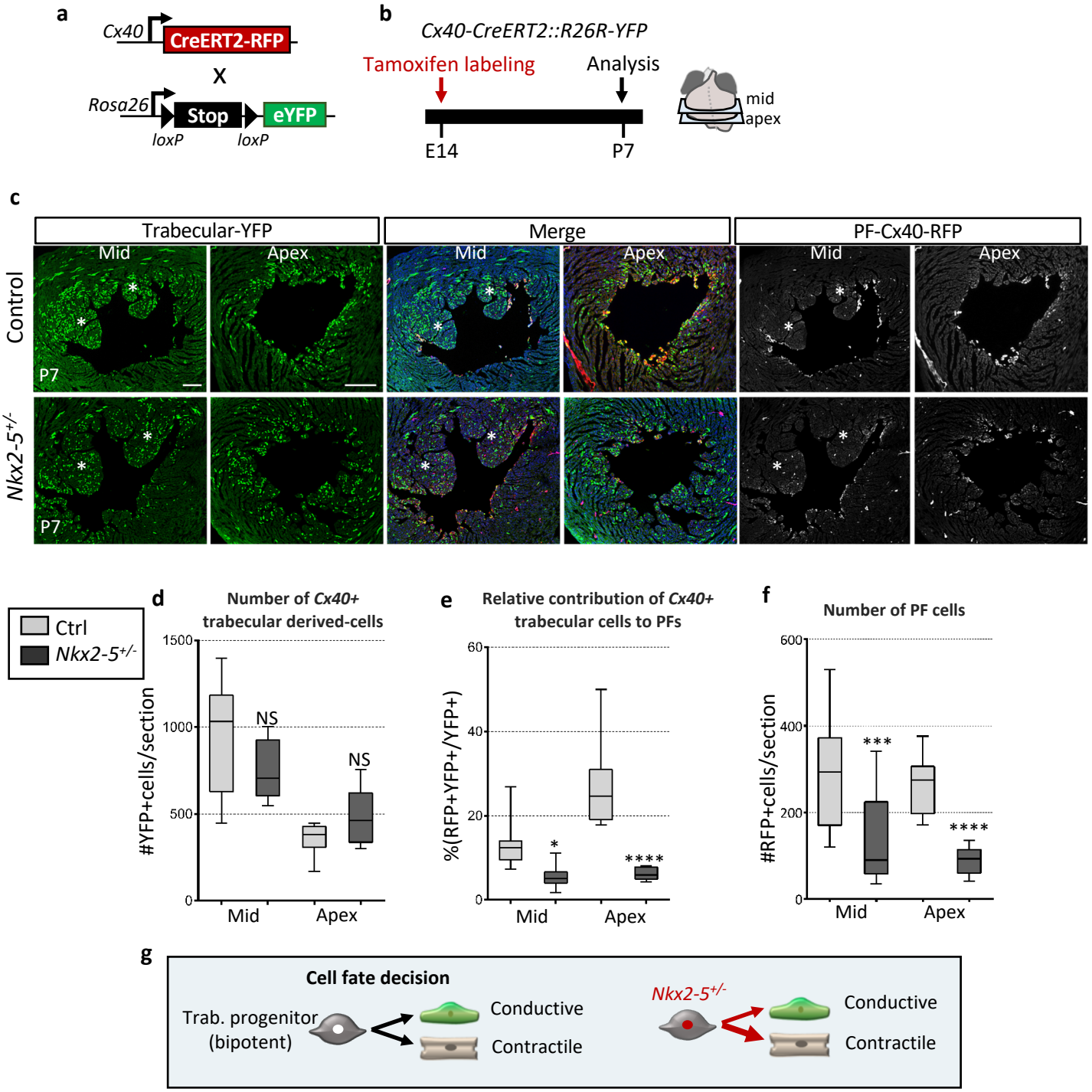

Fig. 1: Defective contribution of *Cx40+* derivative trabecular cells to the postnatal PF in *Nkx2-5*$^{+/-}$ mice. **a,** Scheme of the strategy used for genetic lineage tracing of *Cx40+* cells. *R26R-YFP* reporter mouse line are crossed with tamoxifen inducible *Cx40-CreERT2* mice. Injection of tamoxifen induces the recombination of loxP sites resulting in the expression of the fluorescent protein YFP in *Cx40+* cells. **b,** Tamoxifen is injected at E14 and *Cx40+* derivative cells are analyzed at P7. **c,** Immunostaining for YFP and RFP on *Cx40-CreERT2-RFP::R26R-YFP* control (ctrl) or *Nkx2-5*$^{+/-}$ heart transverse sections at P7, shows distribution of *Cx40+* derivative cells (YFP+) and their fate into PFs (YFP+RFP+). Asterisks represent papillary muscles; scale bars=200µm. **d-f,** Graphs of quantifications from (c) images. The total number of trabecular derived cells (YFP+) per section **(d)**, the relative contribution of trabecular cells to PFs ((YFP+RFP+)/YFP+) **(e)** and the total number RPF cells (RFP+) **(f)** are quantified in mid and apical sections. 3 sections/heart; N=4. *P* values are derived ordinary one-way ANOVA test,* *P*<0,05. NS: non significant. **g,** Scheme illustrating the differentiation of embryonic trabecular progenitors into conductive and contractile cardiomyocytes. In *Nkx2-5*$^{+/-}$ mice, the cell fate decision into conductive cardiomyocytes is disturbed and haploinsufficient trabecular progenitors mostly give rise to contractile cardiomyocytes.

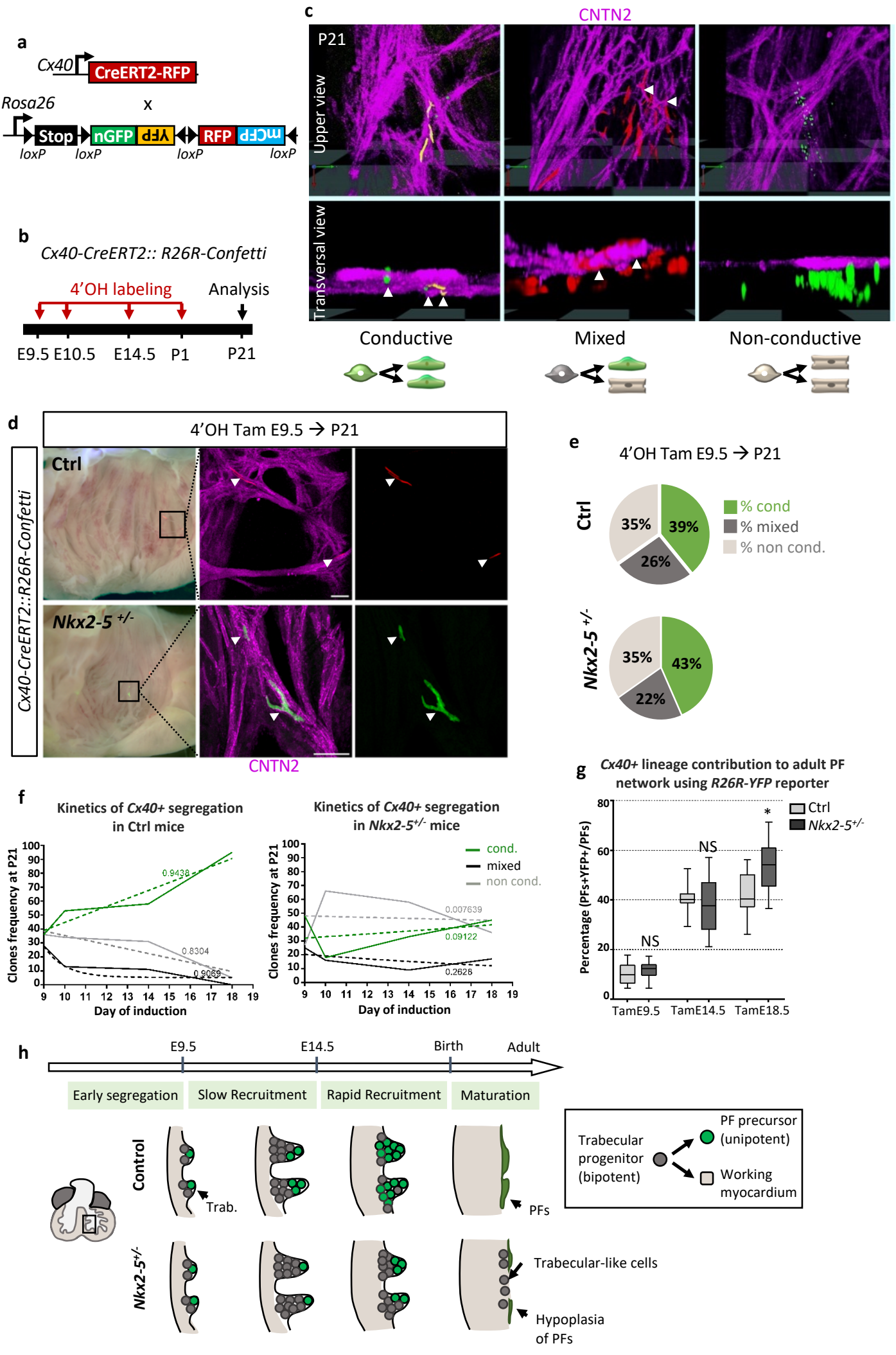

Fig. 2: Temporal clonal analysis of single *Cx40+* trabecular cells during embryonic stages. a, Scheme of the strategy used for clonal genetic tracing of *Cx40+* cells. *R26R-Confetti* multicolor reporter mice are crossed with tamoxifen-inducible *Cx40-CreERT2* mice. Four alternative recombination (nGFP, YFP, RFP, and mCFP) are possible. **b,** Low doses of 4-hydroxytamoxifen (4'OH-Tam) are injected at different time points of development to induce low-frequency recombination. Analyses of independent unicolor clones are made at P21. **c,** 3D reconstructions of clones imaged at the subendocardial surface of the left ventricle. Whole-mount immunostaining for Contactin-2 (CNTN2) is used to distinguish conductive, mixed and non-conductive clones. Arrows indicate cells positive for CNTN2. Schemes illustrate the lineage origin of each clones. **d,** Confocal images of whole-mount CNTN2-immunostaining of 3 week-old *Cx40-CreERT2::R26R-Confetti* opened-left ventricle induced at E9.5 from control (Ctrl) and *Nkx2-5*$^{+/-}$ hearts. Conductive clones are indicated by arrowheads. Scale bars=100µm. **e,** Percentages of conductive, mixed and non conductive clones induced at E9.5 were quantified in P21 control (Ctrl) and *Nkx2-5*$^{+/-}$ left ventricles. **f,** Clones frequency evolution upon time-course inductions quantified in P21 control (*Ctrl)* and *Nkx2-5*$^{+/-}$ mice. The progressive decrease of mixed clones frequency over time illustrates the kinetics of *Cx40+* trabecular progenitors segregation. Dashed lines: non linear regression curves. With R square values. **g,** Graphs of the percentage of labelled adult PFs according to *Cx40+* lineage traced by Tam injections at E9.5, E14.5 or E18.5. Quantifications are made on *Cx40-CreERT2::R26R-YFP* control (ctrl) or *Nkx2-5*$^{+/-}$ heart transverse sections. 3-4sections/heart; N=3-4. *P* values are derived ordinary one-way ANOVA test (Tukey test),* *P*<0,05. NS: non significant. **h,** Model of the progressive segregation of *Cx40+* trabecular progenitors toward the conduction lineage. In control mice, the bipotent *Cx40+* trabecular progenitors (dark grey cells) segregate individually toward conductive and working lineages along development. From E9.5 a subset of progenitors is already fated to the conductive lineage (green cells). During embryonic stages, trabecular progenitors are slowly recruited into the conductive lineage, whereas during fetal stages their recruitment is rapid. After birth, the segregation of trabecular progenitors is accomplished and unipotent *Cx40+* cells participate either to the PF network or working myocardium. In *Nkx2-5*$^{+/-}$ mice, *Cx40+* trabecular progenitors fail to differentiate into conductive cells resulting in a hypoplastic PF network and an abnormal presence of trabecular-like cells.

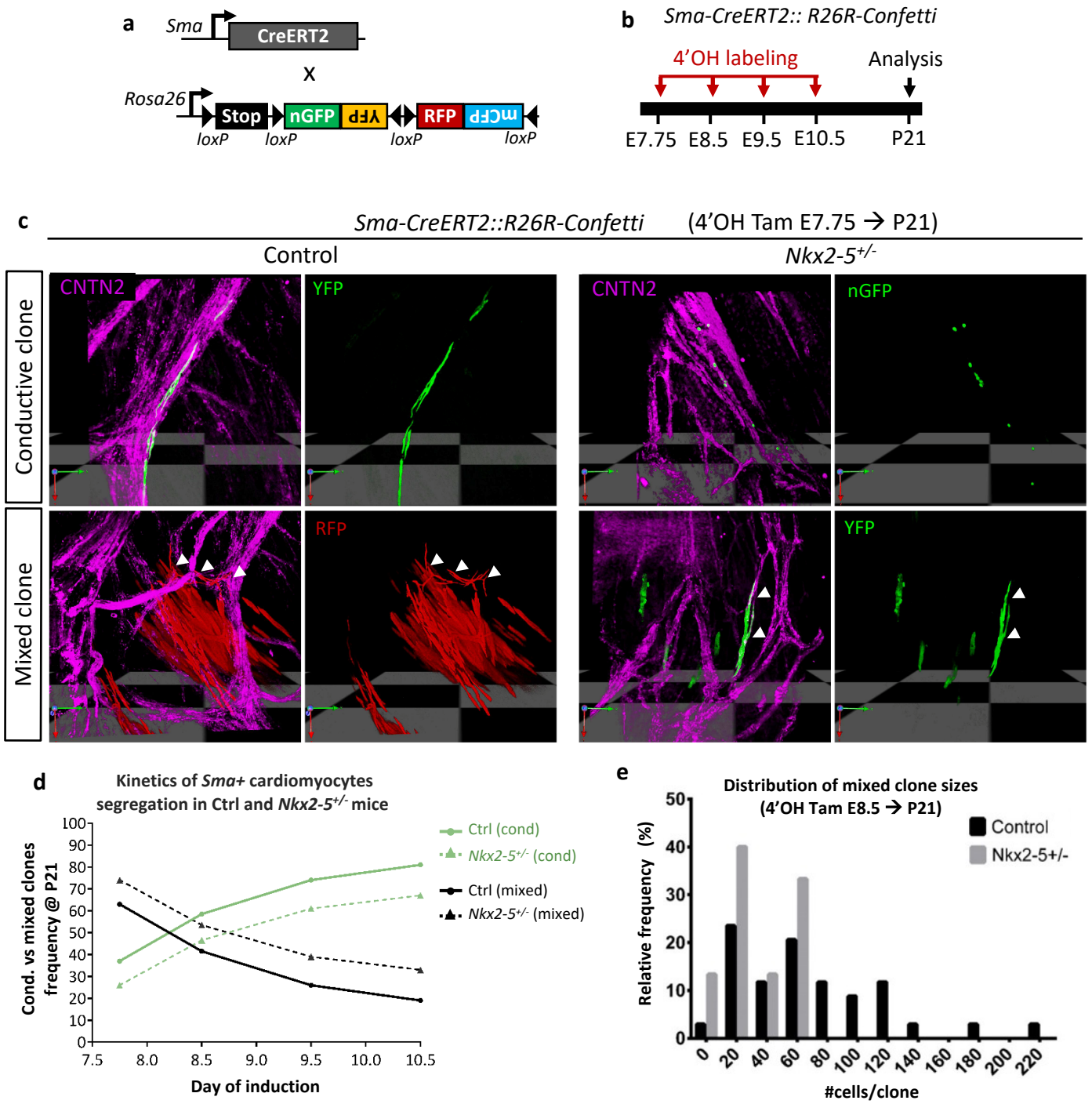

Fig. 3: Temporal clonal analysis of single *Sma+* cardiomyocytes during embryonic stages. a, Scheme illustrating the genetic clonal tracing strategy using *R26R-Confetti* multicolor reporter mouse line crossed with tamoxifen-inducible *Sma-CreERT2* mice. **b,** Time course of 4-hydroxytamoxifen (4'OH-Tam) injections and analyses of independent unicolor clones represented on a time scale. Low doses of 4'OH induce low-frequency recombination. **c,** 3D reconstructions of conductive and mixed clones induced at E7.75 and observed within *Sma-CreERT2::R26R-Confetti* opened-left ventricles at P21 of control (Ctrl) and *Nkx2-5*$^{+/-}$ left ventricle. Whole-mount immunostaining for Contactin-2 (CNTN2) is used to distinguish conductive cells (CNTN2+) as indicate by arrowheads. **d,** Conductive versus mixed clones frequency evolution upon time-course inductions quantified in P21 control (*Ctrl)* and *Nkx2-5*$^{+/-}$ left ventricle. The progressive decrease of mixed clones frequency over time illustrates the kinetics of *Sma+* cardiac progenitors segregation. **e,** Diagram of the relative frequency of mixed clone sizes induced at E8.5 in P21 control and *Nkx2-5*$^{+/-}$ left ventricles.

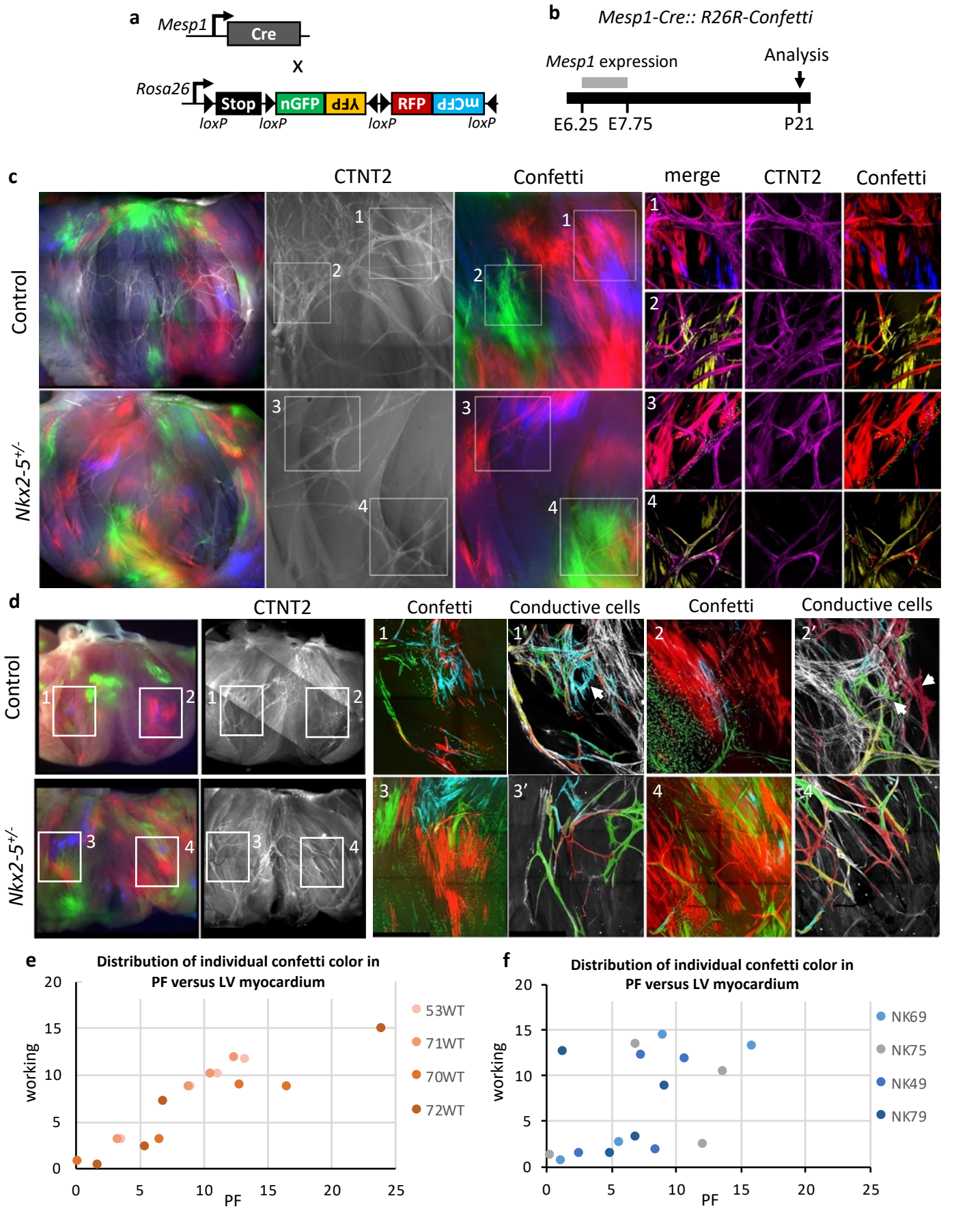

Fig. 4: Mosaic tracing analysis of *Mesp1+* early cardiac progenitors. a, Scheme illustrating the genetic tracing strategy using *R26R-Confetti* multicolor reporter mouse line crossed with non-inducible *Mesp1-Cre* mice. **b,** Recombination of the confetti allele occurs during the short time-window of *Mesp1* expression, between E6.25 and E7.75. Mosaic tracing analysis in control and *Nkx2-5*$^{+/-}$ mice is performed at P21. **c,** Whole-mount fluorescence views of *Mesp1-Cre::R26R-Confetti* opened-left ventricles at P21. Immunostaining for Contactin-2 (CNTN2) is used to label the mature PF network. Small panels (1 to 4) are high magnified confocal images of different PF network regions. **d,** Small panels (1-4) are high magnified confocal images of PF network. Panels (1'-4') are image reconstructions in which only conductive confetti+ cells are manually drawn. The non-conductive confetti+ cells are not represented. In control hearts, the conductive confetti+ cells form either small or large monochromatic clusters. Large clusters (arrows) contribute to complex parts the PF network. In *Nkx2-5*$^{+/-}$ hearts, only small clusters contribute to the hypoplastic network. **e-f,** Dot plots of individual *Mesp1+* confetti colors percentage contribution to the working myocardium versus PF network in control (WT) or *Nkx2-5*$^{+/-}$ (NK) hearts.

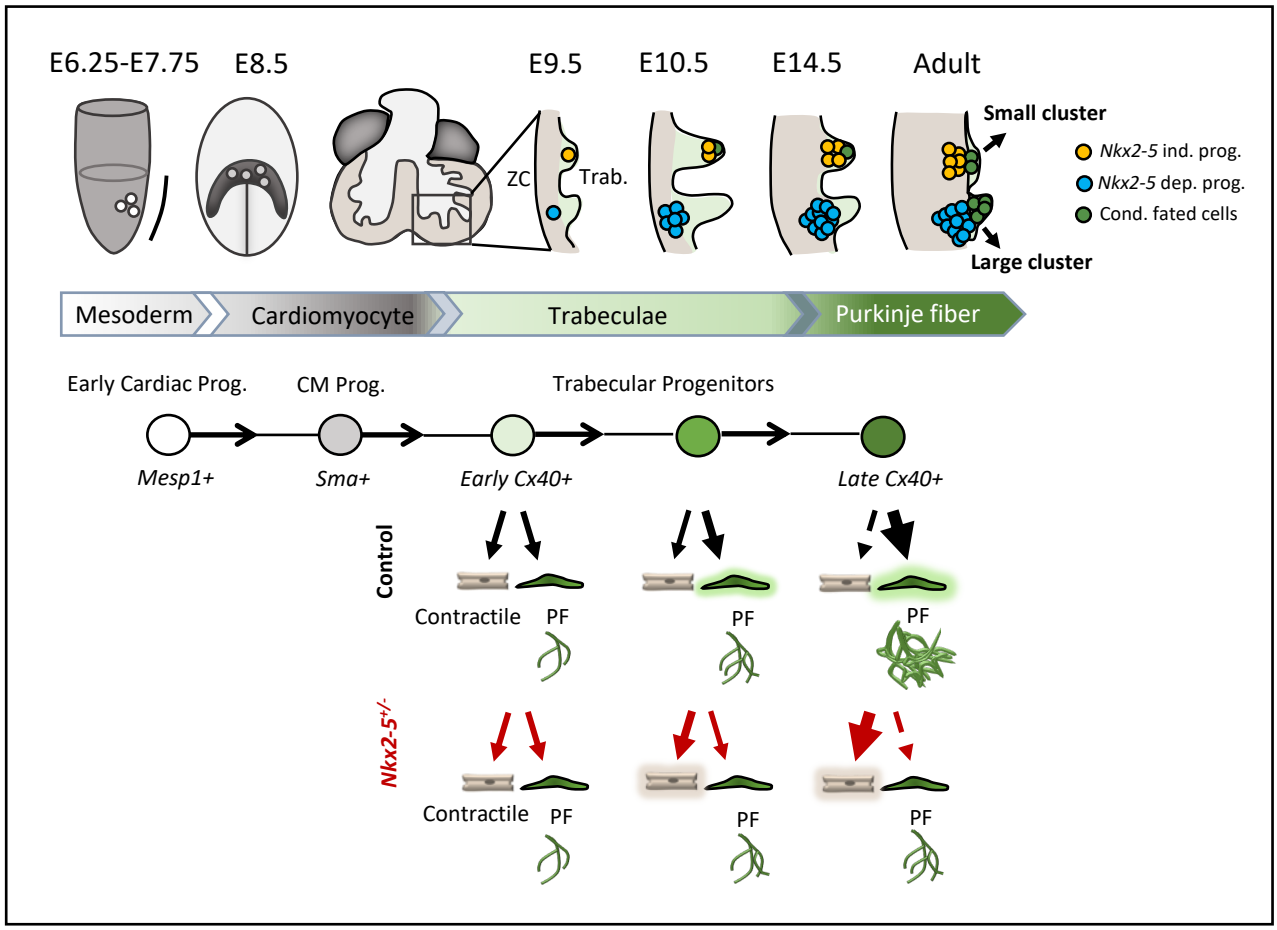

Fig. 5: Model of the Purkinje fiber lineage segregation and temporal requirement of *Nkx2-5* during PF network morphogenesis. Scheme represents the contribution of temporal progenitor cells and their ability to form PF network structures. In gastrulating embryo, a population of *Mesp1*+ progenitors that are engaged into the cardiomyocyte lineage (*Sma+*) will contribute to the ventricular myocardium. During trabeculation (Trab.), a subpopulation is quickly engaged into the *Cx40*+ lineage (yellow cells). This segregation is accompanied by a reduction of proliferative behavior which give rise to small clusters building a polyclonal PF network. This subpopulation of progenitors are *Nkx2-5*-independent. Besides, a high proliferative subpopulation (blue cells) with similar cell behavior with compact myocardium (ZC), segregates at late fetal stage into the conductive lineage and is *Nkx2-5-dependent*. This produces large clusters that massively participate to ellipsoidal structures of the PF network. In control mice the conductive potency of *Cx40*+ trabecular progenitors increases with time, whereas in *Nkx2-5*$^{+/-}$ mice, the conductive potency is progressively lost leading to very rare large clusters, the major cause of hypoplastic network phenotype.

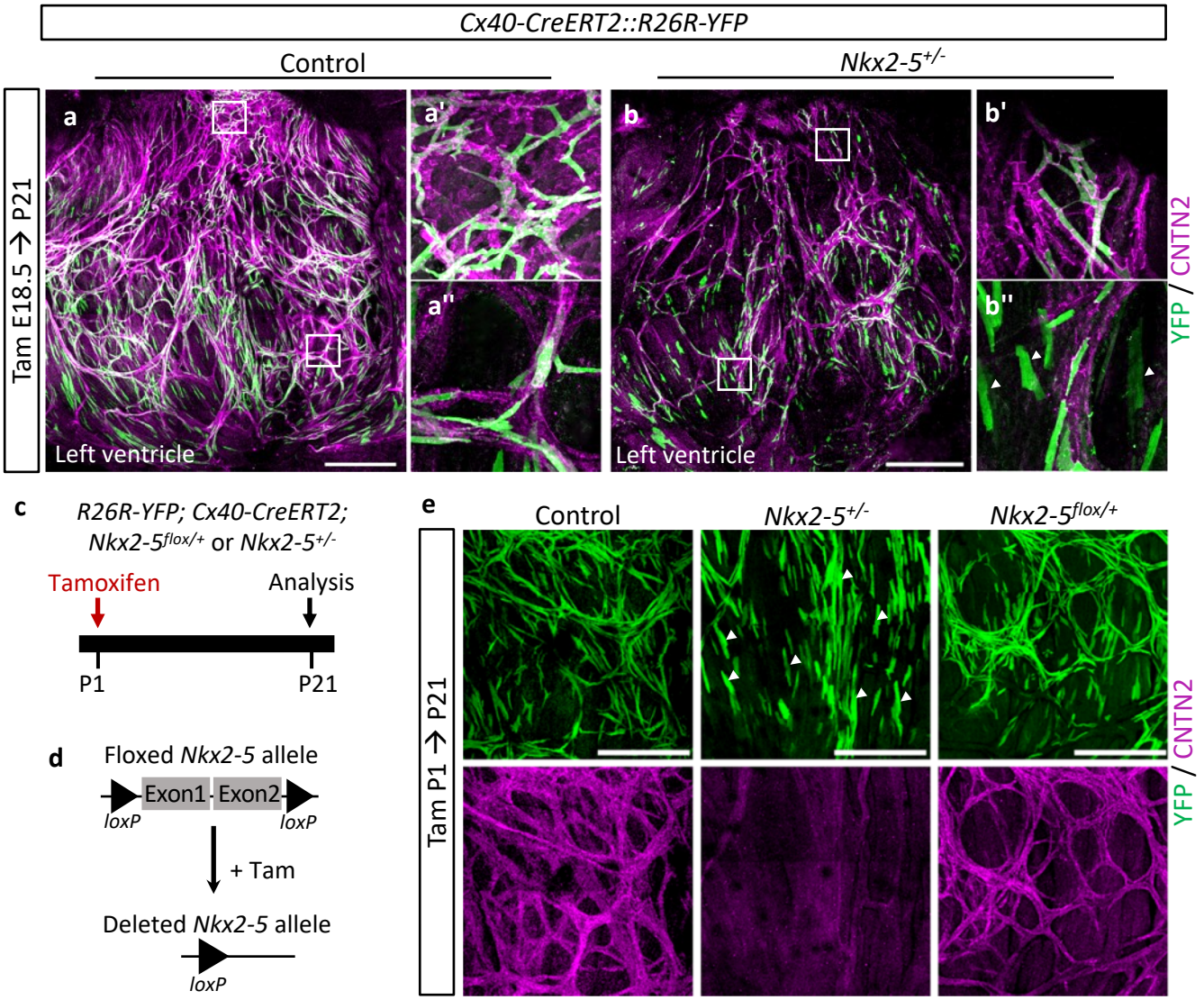

Fig. 6: Purkinje network morphogenesis has occurred at birth and is maintained in *Nkx2-5*$^{+/-}$ hearts. a-e, Genetic tracing of Cx40+ cells labeled at E18.5 by Tam injection. Confocal images of whole-mount CNTN2-immunostaining of *Cx40-CreERT2::R26R-YFP* opened-left ventricle at P21. **a-b'',** Immunostaining for YFP and CNTN2 on control, or *Nkx2-5*$^{+/-}$ mice shows E18.5 *Cx40+* derived-cells that participate to the PF network. Scale bars=1mm; **(a'-b')** are high magnifications of left bundle branch; **(a''-b'')** are high magnifications of PF. **c-d,** Strategy to induce conditional deletion of one copy of *Nkx2-5* allele (*Nkx2-5*$^{flox/+}$) using *Cx40-CreERT2* line as inducible Cre driver. Deletion is performed at P1 when *Cx40+* cells are mostly PF cells. *R26R-YFP* reporter line is used to compare the tracing of P1 *Cx40+* derived-cells within P21 *Nkx2-5*$^{+/-}$ and *Nkx2-5*$^{flox/+}$ hearts. e, Confocal imaging of left PF network. Scale bars=500µm; arrowheads indicate non-conductive *Cx40+* derived-cells.

a

	4'OH E9.5		4'OH E10.5		4'OH E14.5		4'OH E18.5	
	Ctrl	*Nkx2-5$^{+/-}$*	Ctrl	*Nkx2-5$^{+/-}$*	Ctrl	*Nkx2-5$^{+/-}$*	Ctrl	*Nkx2-5$^{+/-}$*
total hearts	10	15	16	10	8	9	6	4
total clones	36	48	64	50	118	128	105	58
frequency/ heart	3,6	3,2	4	5	14,75	14,2	17,5	14,5
% GFP+	39,1	30,4	37,5	44	39,3	37,5	34,3	37,9
% CFP+	4,3	4,3	1,6	2	0,85	0	0,95	0
% RFP+	43,5	52,2	42,2	40	38,5	41,4	45,7	43,1
% YFP+	13,0	13,0	18,75	14	21,4	21,1	19,0	19,0
% cond. clones	36,1	47,9	53,1	18	57,6	32,8	95,2	44,8
% mixed clones	27,8	25	12,5	16	11,0	9,4	0	17,2
% non-cond. clones	36,1	27,1	34,4	66	37	57,8	5	36,2
size cond. clones	5,4	5,1	4,5	3,9	2,6	2,5	3,18	1,9
size mixed clones	27,7	13,3	31,1	9,25	6,5	7,25	0	6
size non-cond. clones	16,9	27,7	31,6	16,1	6,5	6,7	4,8	3,0

b

	4'OH E7.75		4'OH E8.75		4'OH E9.5		4'OH E10.5	
	Ctrl	*Nkx2-5$^{+/-}$*	Ctrl	*Nkx2-5$^{+/-}$*	Ctrl	*Nkx2-5$^{+/-}$*	Ctrl	*Nkx2-5$^{+/-}$*
total hearts	4	4	13	5	20	14	5	8
total clones	19	19	82	28	179	64	37	48
Frequency/ LV	4,75	4,75	6,3	5,6	9,0	4,6	7,4	6,0
% cond. clones*	37	26	58,5	46,4	73,7	60,9	81,1	66,7
% mixed clones*	63	74	41,5	53,6	26,3	39,1	18,9	33,3
size cond. clones	15,7	10,5	9,4	5,4	10,2	10,4	7,0	5,8
size mixed clones	156,25	96,1	68,6	32,7	47,5	39,8	72,4	31,9
size cond. in mixed	20,4	13,1	24,1	7,5	14,1	10,7	7,3	4,5

Table 1: Quantitative analysis of *Cx40+* and *Sma+* derived-clones. a, Table represents the n values of hearts and clones analyzed in this study, using *Cx40-CreERT2*::*R26R-Confetti* mouse line. Only clones observed in the subendocardial surface of the inter-ventricular septum within the left ventricle are analyzed. Percentages of colors and type of clones are represented. The size of clones are measured by quantifying the number of cells per clone. **b,** Table represent the same quantifications using *Sma-CreERT2*::*R26R-Confetti* mouse line. Asterisks shows percentages of conductive clones versus mixed clones. Non-conductive clones are excluded from the analysis.